Nickel(II) Complexes with Unsymmetrical Quadridentate Schiff Bases having a Pendant *N*-Acyl Substituent†

Marek Kwiatkowski *[a] **and Giuliano Bandoli**[b]

[a] *Institute of Chemistry, University of Gdańsk, Sobieskiego 18, 80952 Gdańsk, Poland*

[b] *Department of Pharmaceutical Sciences, University of Padua, via F. Marzolo 5, 35131 Padua, Italy*

The condensation of *N*-acylated derivatives of *o*-aminocarbonyl aromatic compounds with the precursor 7-amino-4-methyl-5-azahept-3-en-2-one has been found to depend on the acidity of the amide proton and the nature of the substituent on the carbonyl carbon atom. Three new quadridentate Schiff-base ligands and their nickel(II) complexes having a pendant *N*-acetyl or *N*-trifluoroacetyl group have been obtained and characterized by spectroscopic techniques. A very unusual temperature-dependent proton NMR spectrum has been found for [4-methyl-9-(*o*-trifluoroacetylaminophenyl)-5,8-diazadeca-3,8-dien-2-onato(2−)]nickel(II) indicating a substantial energy barrier for enantiomer interconversion of the chiral complex molecule at moderate temperature. The crystal and molecular structure of this complex has been determined and shows that a fluorine–nickel interaction may be responsible for the inhibited enantiomer interconversion in *N*-trifluoroacetyl substituted nickel complexes. Crystallographic data: space group $P2_1/c$, a = 9.057(2), b = 13.769(4), c = 14.664(4) Å, β = 108.43(2)°, final R = 0.0434.

Since the first reports on the synthesis of 7-amino-4-methyl-5-azahept-3-en-2-one **1** [1,2] the compound has been widely used as a precursor for the preparation of unsymmetrical quadridentate Schiff-base ligands **3** by simple condensation of its primary amino group with the carbonyl group in *ortho*-substituted aromatic carbonyl compounds **2**.[1–6] Our recent studies [3,4] have shown that the formation of compound **3** is sensitive to the nature of the substituents X and R in **2**. The presence of an acidic hydrogen atom on the X substituent facilitates the reaction while bulkier and/or electron-donating R groups have the opposite effect. For example, when X = OH the intramolecular hydrogen bond between the fairly acidic phenolic hydrogen and the carbonyl oxygen atom in **2** catalyses the condensation with **1** so effectively that corresponding ligands **3** are formed in excellent yield, regardless of R (R = H, CH_3, or C_6H_5).[1] On the other hand, when X = NH_2 such catalysis is less efficient owing to the far less acidic properties of the amino hydrogen atoms. A methyl or phenyl group R inhibits the reaction entirely in this case; only the derivative with R = H can be obtained and only in the form of a complex with a divalent metal ion.[3]

We were interested to see whether an increase in the acidic properties of a nitrogen-bonded hydrogen atom in **2** upon introducing electron-withdrawing *N*-acyl substituents would enhance the reactivity of **2** towards the precursor **1**. In this paper the reaction of **1** with *N*-acetyl and *N*-trifluoroacetyl derivatives of 2-aminobenzaldehyde, 2-aminoacetophenone and 2-aminobenzophenone is reported. Three new unsymmetrical quadridentate Schiff-base ligands of the N_3O type, and their nickel(II) complexes, have been prepared. The single-crystal X-ray structure of one of the complexes, [4-methyl-9-(*o*-trifluoroacetylaminophenyl)-5,8-diazadeca-3,8-dien-2-onato-(2−)]nickel(II), has been determined.

Results and Discussion

The reaction of *N*-acetyl and *N*-trifluoroacetyl derivatives of 2-amino-benzaldehyde, -acetophenone, and -benzophenone with the precursor **1** (1 h reflux in methylene chloride) was monitored by means of field desorption (FD) mass spectrometry. The results, when compared to a similar study [3] on the non-acylated derivatives, show that the reactivity towards **1** follows generally the increase in NH proton acidity NH_2 < $NHCOCH_3$ < $NHCOCF_3$. This increase accounts for the more efficient intramolecular hydrogen bonding to the carbonyl oxygen atom and, consequently, for the reduced electron density on the carbonyl carbon atom facilitating nucleophilic attack of the primary amino group of **1**. Thus, the crystalline unsymmetrical ligands **4a**, **4b**, and **4c** were obtained by the reaction of **1** with 2-*N*-acetylaminobenzaldehyde, 2-*N*-trifluoroacetylaminobenzaldehyde and 2-*N*-trifluoroacetylaminoacetophenone, respectively, while 2-*N*-acetylaminoacetophenone yielded an equilibrium mixture containing both the unsymmetrical product and unchanged precursors. The benzophenone derivatives were entirely unreactive towards **1**, as the increase in NH proton acidity apparently cannot outweigh the electron-donating properties of the additional phenyl ring which increase the electron density at the site of nucleophilic substitution, thus inhibiting the condensation.

† *Supplementary data available:* see Instructions for Authors, *J. Chem. Soc., Dalton Trans.*, 1992, Issue 1, pp. xx–xxv.

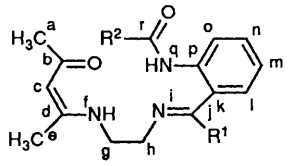

	R^1	R^2
4a	H	CH_3
4b	H	CF_3
4c	CH_3	CF_3

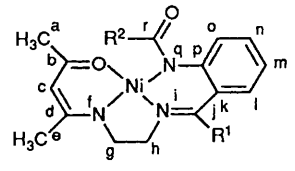

	R^1	R^2
5a	H	CH_3
5b	H	CF_3
5c	CH_3	CF_3

Elemental analysis, FD mass and proton NMR spectroscopic data for the three crystalline ligands **4a**–**4c** are fully consistent with the structures depicted. In the NMR spectra of the ligands and their acylamino carbonyl precursors the doublet of aromatic proton H°, next to the acylamino substituent, is observed at unusually low field at δ 8.7. A similarly high chemical shift (δ 8.7) has been reported for *N*-acetylanthranilic acid,[7] while the usual chemical shift range for such protons in monosubstituted *N*-acylaminobenzenes is δ 7.3–7.6.[7] This deshielding is evidently related to the presence of a substituent *ortho* to the acylamino group, capable of forming a hydrogen bond to the amide hydrogen atom. Apparently, this intramolecular hydrogen bonding to imino, carbonyl, or carboxyl groups tends to render the amide moiety in a coplanar arrangement with respect to the phenyl ring, placing the amide C=O group, a local centre of magnetic anisotropy, in the vicinity of the aromatic proton H°, hence deshielding. As usual in unsymmetrical ligands derived from the precursor **1**, the enamine hydrogen proton H^f is coupled to the methylene protons H^g with $J(H^fH^g)$ *ca.* 6 Hz.

The ligands **4a**–**4c** readily react with nickel(II) acetate tetrahydrate to give the corresponding nickel(II) complexes **5a**–**5c**, respectively, as orange to red-brown crystalline solids. The complexes are neutral, *i.e.* the charge of the nickel(II) ion is entirely neutralized by the dinegative quadridentate anion originating from loss of one amide and one enamine proton from the ligand molecule. In the fast atom bombardment (FAB) mass spectra of the complexes characteristic clusters of peaks resulting from superimposition of $[M]^+$ and $[M + 1]^+$ peaks, each in turn split into components due to the natural abundance of the nickel isotopes, are observed. The fragmentation is marginal and involves loss of R^2 and R^2CO fragments from the *N*-acyl substituent. The latter fragmentation pathway indicates that the amide oxygen is not engaged in co-ordination of the central ion and that nickel is bound by the amide nitrogen atom.

In the UV/VIS spectra of complexes **5a**–**5c** the d–d transition appears as a shoulder at 450–490 nm, extending into the visible region. No absorption above 660 nm and the diamagnetism of the complexes indicate a square-planar geometry around the nickel ion.[8] Several IR absorption bands in the 1500–1600 cm^{-1} region (Table 1) can be attributed to the C=O, C=N, and C=C stretching vibrations of the co-ordinated ligand molecule. The C=O stretch of the unco-ordinated amide gives rise to a strong band at 1630–1640 cm^{-1}.

Proton NMR spectral data for complexes **5a**–**5c** are given in Table 1. Lack of the low-field NH resonance is consistent with the structures depicted, wherein the ligand molecule is doubly deprotonated. The resonance of the methine proton H^{R^1} is shifted 0.9–1.0 ppm upfield with respect to the corresponding signal of the free ligands, reflecting the overall conformational change of the complexed ligand (the chemical shift of H^{R^1} was reported to be the most conformation-sensitive in this type of compound[4]). The doublet of the aromatic proton H° is shifted 0.48–0.77 ppm upfield upon complexation, while the rest of aromatic resonances do not experience any definite shift. Obviously, in the nickel complex the amide group can be no longer rendered coplanar to the aromatic ring, as this would require the substituent R^2 to approach too close to the co-ordinating carbonyl oxygen atom (model studies reveal that in the hypothetical strictly coplanar arrangement the distance between the carbon atom of R^2 and the co-ordinating oxygen atom would be *ca.* 2.2 Å, that is 1.0 Å shorter than the sum of the van der Waals radii,[9] and still there is the contribution of the R^2 hydrogen or fluorine atoms to the repulsive forces). Therefore, the deshielding by the aromatic hydrogen atoms described for the free ligands (see above) is less effective for the nickel complex. The 0.9 ppm downfield shift of the *N*-acetyl methyl resonance (δ 2.03 for **4a**, 2.93 for **5a**) indicates that even when the amide group is bent out-of-plane the R^2 substituent is still close to the deshielding C^b=O fragment.

Two methylene groups g and h give rise to two triplets in the proton NMR spectra of complexes **5a** and **5b**. This pattern, observed as a rule for a number of related diamagnetic unsymmetrical complexes,[1–5,10] arises from the simple coupling between two adjacent pairs of magnetically equivalent protons with a single coupling constant $J(H^gH^h)$ 6.1–6.3 Hz. Again, the triplets are shifted upfield by 0.4–0.6 ppm with respect to the corresponding signals of the free ligands, and they are more separated (the resonance of methylene group g of the free ligands appears as a quartet due to the additional coupling to the enamine proton H^f with virtually the same coupling constant). In the case of complex **5c** the spectrum of the ethylene fragment is remarkably different. Instead of two triplets composed of narrow resonance lines, three broad features of intensity 1:1:2 are observed at room temperature in $CDCl_3$ solution (Table 1). This pattern seems not to be solvent-dependent as it is also observed in $(CD_3)_2SO$ and C_5D_5N solution (the compound is very poorly soluble in other common organic solvents). The spectra from −27 to 80°C in C_5D_5N (a solvent of choice for this temperature range) showed a marked temperature dependence (Fig. 1), indicating the presence of some dynamic process inhibited at low temperature. Below −15 °C a complex ABCD type subspectrum is observed with chemical shifts of δ 2.42, 2.98, 3.41, and 3.45 for H^g, $H^{g'}$, H^h, and $H^{h'}$, respectively. As the last two signals overlap and the signal-to-noise ratio is low at low temperature due to reduced solubility, no coupling constants can be determined. As the temperature rises, the signals broaden, coalesce, and finally form an almost completely averaged spectrum with $\bar{\delta}_g$ = 2.773, $\bar{\delta}_h$ = 3.446, and $\bar{J}(H^gH^h)$ = 6.2 Hz at 80 °C.

A close inspection of the triplets in the spectrum of complex **5b** shows some broadening of the components. Lowering the temperature to −40 °C causes a change in this pattern (Fig. 2), though even at −55 °C the hyperfine structure only starts to appear in $CDCl_3$ solution. A more detailed variable-temperature study of this compound has not been performed due to its extremely low solubility at low temperature. No change in the triplet–triplet pattern in the spectrum of **5a** was observed down to −50 °C.

Carbon-13 NMR spectral data for the complexes are given in Table 1. The assignment of most resonances to the appropriate carbon atoms is quite straightforward, and the spectra are consistent with the structures **5a**–**5c**. The resonances

Table 1 Infrared and NMR spectroscopic data for the nickel complexes

Compound	IR[a] (cm^{-1})	NMR (δ)[b] ^1H[c]	^{13}C
5a	1512s 1540s 1567s 1602s 1640m	1.832, 1.916 (s, $H^{a,e}$), 2.914 (t, H^g), 2.928 (s, H^{R^2}), 3.299 (t, H^h), 4.990 (s, H^c), 6.985 (t, H^m), 7.260 (d, H^l), 7.390 (t, H^n), 7.421 (s, H^{R^1}), 7.926 (d, H^o); $J(H^gH^h)$ 6.3, $J(H^lH^m) = J(H^mH^n) = 7.5$, $J(H^nH^o)$ 8.3	23.00, 25.75 ($C^{a,e}$), 30.26 (C^{R^2}), 50.64 (C^g), 62.36 (C^h), 100.61 (C^c), 122.60, 130.30, 132.69, 133.86, 149.16 (aromatic), 164.01 (C^d), 166.40 (C^j), 177.47 (C^b), 178.37 (C^f)
5b	1513s 1582m 1630s	1.814, 1.937 (s, $H^{a,e}$), 2.950 (t, H^g), 3.396 (t, H^h), 5.002 (s, H^c), 7.112 (t, H^m), 7.325 (d, H^l), 7.488 (t, H^n), 7.538 (s, H^{R^1}), 8.267 (d, H^o); $J(H^gH^h)$ 6.1, $J(H^lH^m) = J(H^mH^n) = 7.7$, $J(H^nH^o)$ 8.2, $J(H^lH^n)$ 1.3	21.50, 23.97 ($C^{a,e}$), 49.79 (C^g), 61.13 (C^h), 99.95 (C^c), 122.91, 127.26, 127.56, 131.78, 133.14, 145.23 (aromatic), 163.02 (C^d), 164.96 (C^j), 177.39 (C^b)
5c	1510s 1581m 1630s	1.794, 1.909 (s, $H^{a,e}$) 2.405 (s, H^{R^1}), 2.80 (br, H^g), 3.14 (br, $H^{g'}$), 3.54 (br, H^h), 4.971 (s, H^c), 7.131 (t, H^m), 7.462 (t, H^n), 7.505 (d, H^l), 7.973 (d, H^o); $J(H^lH^m) = J(H^mH^n) = 7.7$, $J(H^nH^o)$ 8.1	18.52, 21.10, 24.02 (C^{a,e,R^1}), 50.81 (C^g), 55.26 (C^h), 99.09 (C^c), 122.88, 127.60, 127.82, 131.88, 143.46 (aromatic), 164.49 (C^d), 170.06 (C^j), 177.43 (C^b)

[a] s = Strong, m = medium. [b] In $CDCl_3$ solution, $SiMe_4$ as internal reference; J in Hz. [c] s = Singlet, d = doublet, t = triplet, and br = broad.

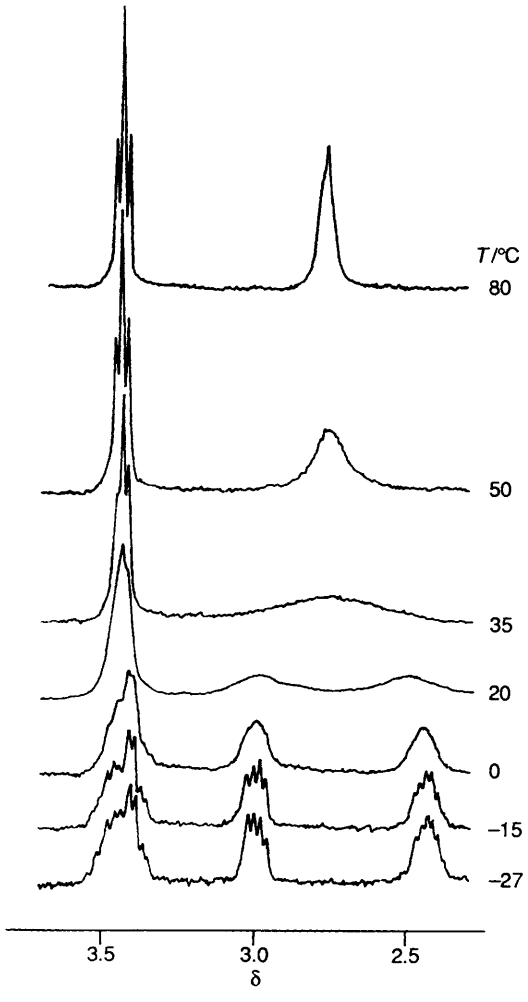

Fig. 1 Proton NMR resonances of methylene groups g and h in complex **5c** at various temperatures in C_5D_5N solution with $SiMe_4$ as internal reference

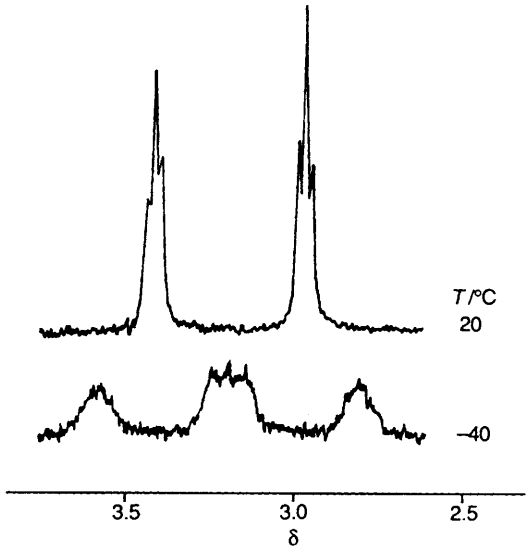

Fig. 2 Proton NMR resonances of methylene groups g and h in complex **5b** at 20 and −40 °C in $CDCl_3$ solution with $SiMe_4$ as internal reference

of the CF_3CO substituents in **5b** and **5c** are not detected above the noise level. Evidently, the low efficiency of the relaxation mechanisms for quaternary carbon atoms, the splitting due to coupling to fluorine and the poor solubility of the complexes contribute to the overall low intensity of these signals. No unusual shifts are observed for the methylene carbons C^g and C^h of the ethylene moiety in **5b** and **5c**.

The unusual temperature dependence of the proton NMR spectrum of the ethylene fragment in complexes **5b** and **5c** seems to be related to the presence of a pendant *N*-trifluoroacetyl substituent. So far, no mononuclear nickel(II) complex with an unsymmetrical Schiff base of type **3** has been reported to show a similar effect. For example, the proton NMR spectrum of the nickel complex with the ligand **3** (R = H, X = OH, Y = H) had been studied down to −60 °C in $CDCl_3$ solution[10] and no substantial change in the triplet–triplet pattern had been observed. In a search for a plausible

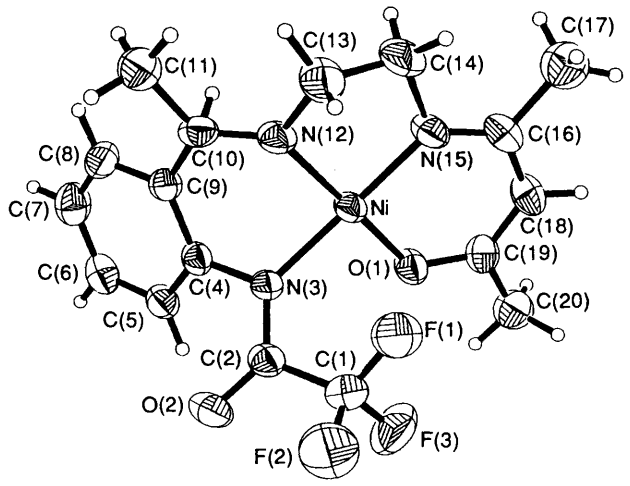

Fig. 3 Perspective view of complex **5c** including the atom numbering scheme

Table 2 Fractional atomic coordinates ($\times 10^4$) for complex **5c**

Atom	*x*	*y*	*z*
Ni	1363(1)	1470(1)	4590(1)
O(1)	1564(3)	1601(2)	5869(2)
O(2)	1309(4)	4453(2)	4524(2)
C(1)	3343(5)	3429(3)	5345(3)
F(1)	3977(3)	2578(2)	5247(2)
F(2)	4271(3)	4109(3)	5198(3)
F(3)	3443(3)	3489(3)	6273(2)
C(2)	1652(4)	3593(3)	4694(3)
N(3)	794(3)	2804(2)	4369(2)
C(4)	−738(4)	2960(3)	3745(3)
C(5)	−1731(5)	3630(3)	3959(3)
C(6)	−3256(5)	3737(3)	3359(3)
C(7)	−3801(5)	3171(3)	2535(3)
C(8)	−2817(5)	2532(3)	2309(3)
C(9)	−1276(5)	2405(3)	2902(3)
C(10)	−244(5)	1724(3)	2610(3)
C(11)	−542(5)	1541(3)	1557(3)
N(12)	875(4)	1310(2)	3267(2)
C(13)	1905(6)	589(3)	3046(3)
C(14)	2099(6)	−216(3)	3764(3)
N(15)	2159(4)	217(2)	4692(2)
C(16)	2705(5)	−286(3)	5483(3)
C(17)	3337(6)	−1299(4)	5458(4)
C(18)	2722(5)	74(3)	6389(3)
C(19)	2167(5)	961(3)	6531(3)
C(20)	2225(5)	1271(3)	7527(3)

explanation as to how the trifluoroacetyl substituent can affect the spectrum of the quite remote ethylene fragment, the crystal and molecular structure of complex **5c** was determined.

A perspective view of the molecule is shown in Fig. 3, while the final atomic coordinates, bond distances and angles are given in Tables 2 and 3, respectively. The crystal structure consists of discrete monomeric neutral complex molecules, with no significant intermolecular interactions. The quadridentate ligand is doubly deprotonated at the enamine and amide nitrogen atoms, and binds nickel(II) ion through three nitrogen (enamine, imine, and amide) and one oxygen carbonyl atom. The geometry of metal co-ordination sphere is distorted square planar and the nickel bonding distances and angles are of the same order as reported for related compounds.[11] The nickel centre resides on the basal ONNN plane, however O(1) and N(12) are 0.29(3) and 0.14(4) Å above, while N(3) and N(15) are 0.12(4) and 0.15(5) Å below, this plane, to give a slight tetrahedral distortion from an idealized square-planar arrangement. The sum of valence angles at the nitrogen atoms is 360° indicating a planar configuration corresponding to sp^2 hybridization.

Table 3 Bond distances (Å) and angles (°) for complex **5c**

Ni–O(1)	1.835(3)	C(6)–C(7)	1.390(6)
Ni–N(3)	1.908(3)	C(7)–C(8)	1.366(7)
Ni–N(12)	1.863(3)	C(8)–C(9)	1.402(5)
Ni–N(15)	1.857(3)	C(9)–C(10)	1.480(6)
O(1)–C(19)	1.297(4)	C(10)–C(11)	1.503(6)
O(2)–C(2)	1.229(5)	C(10)–N(12)	1.289(4)
C(1)–F(1)	1.333(5)	N(12)–C(13)	1.467(6)
C(1)–F(2)	1.320(6)	C(13)–C(14)	1.500(7)
C(1)–F(3)	1.336(6)	C(14)–N(15)	1.471(6)
C(1)–C(2)	1.544(5)	N(15)–C(16)	1.306(5)
C(2)–N(3)	1.332(5)	C(16)–C(17)	1.513(6)
N(3)–C(4)	1.416(4)	C(16)–C(18)	1.413(7)
C(4)–C(5)	1.393(6)	C(18)–C(19)	1.361(6)
C(4)–C(9)	1.402(5)	C(19)–C(20)	1.507(6)
C(5)–C(6)	1.391(5)		
O(1)–Ni–N(3)	90.7(1)	C(6)–C(7)–C(8)	119.5(4)
O(1)–Ni–N(12)	172.3(1)	C(7)–C(8)–C(9)	121.8(4)
N(3)–Ni–N(12)	88.5(1)	C(4)–C(9)–C(8)	118.6(4)
O(1)–Ni–N(15)	95.7(1)	C(4)–C(9)–C(10)	121.6(3)
N(3)–Ni–N(15)	170.1(2)	C(8)–C(9)–C(10)	119.7(3)
N(12)–Ni–N(15)	86.1(1)	C(9)–C(10)–C(11)	118.6(3)
Ni–O(1)–C(19)	125.5(3)	C(9)–C(10)–N(12)	118.9(3)
F(1)–C(1)–F(2)	106.7(4)	C(11)–C(10)–N(12)	122.5(4)
F(1)–C(1)–F(3)	105.7(3)	Ni–N(12)–C(10)	126.7(3)
F(2)–C(1)–F(3)	106.3(4)	Ni–N(12)–C(13)	110.6(2)
F(1)–C(1)–C(2)	116.0(3)	C(10)–N(12)–C(13)	122.7(3)
F(2)–C(1)–C(2)	110.7(3)	N(12)–C(13)–C(14)	106.7(4)
F(3)–C(1)–C(2)	110.8(4)	C(13)–C(14)–N(15)	108.1(4)
O(2)–C(2)–C(1)	113.8(3)	Ni–N(15)–C(14)	113.7(3)
O(2)–C(2)–N(3)	129.1(3)	Ni–N(15)–C(16)	126.3(3)
C(1)–C(2)–N(3)	117.1(3)	C(14)–N(15)–C(16)	119.9(3)
Ni–N(3)–C(2)	128.9(2)	N(15)–C(16)–C(17)	120.5(4)
Ni–N(3)–C(4)	114.3(2)	N(15)–C(16)–C(18)	122.5(4)
C(2)–N(3)–C(4)	116.7(3)	C(17)–C(16)–C(18)	117.0(4)
N(3)–C(4)–C(5)	121.7(3)	C(16)–C(18)–C(19)	124.3(4)
N(3)–C(4)–C(9)	119.0(3)	O(1)–C(19)–C(18)	125.7(4)
C(5)–C(4)–C(9)	119.4(3)	O(1)–C(19)–C(20)	114.2(4)
C(4)–C(5)–C(6)	120.7(3)	C(18)–C(19)–C(20)	120.1(4)
C(5)–C(6)–C(7)	120.0(4)		

The structure comprises three chelate rings, two six- and one five-membered. One six-membered metallocycle involving a pentane-2,4-dione moiety [O(1) to N(15)] is strictly planar and practically coplanar to the co-ordination basal plane (dihedral angle 6.2°). The other six-membered chelate ring [N(3) to N(12)] is in half-boat conformation, the maximum deviation from the six-atom mean plane being +0.41(5) Å for N(3) [−0.37(5) Å for Ni], and the plane is inclined to the basal plane at a dihedral angle of 135.8°. This gives the molecule the characteristic twisted shape (Fig. 4). The five-membered metallocycle comprising the ethylene fragment is in the envelope conformation with deviations from the Ni, N(12), N(15) plane of 0.58(4) and 0.07(2) Å for C(13) and C(14), respectively.

The most interesting feature from the X-ray analysis is the position of the fluorine atom F(1) in the *N*-trifluoroacetyl pendant substituent. The Ni···F(1) distance 2.724(3) Å is significantly shorter than the sum of van der Walls radii (3.0–3.1 Å)[9] indicating the existence of some nickel–fluorine interaction. The F(1)–C(1)–C(2) angle [116.0(3)°] is slightly wider than F(2)–C(1)–C(2) and F(3)–C(1)–C(2) [110.7(3) and 110.8(4)°, respectively] to allow more efficient interaction. The Ni···F(1) line is roughly axial to the basal co-ordination plane [67.9(3)°] resulting in a distorted and axially elongated pseudo-square-pyramidal arrangement (Fig. 4).

The fluorine–nickel interaction is not strong enough at this distance to cause any substantial change in the energies of the nickel(II) d orbitals, and no paramagnetism of complex **5c** has been detected. On the other hand, this interaction is certainly responsible for the observed temperature dependence of the

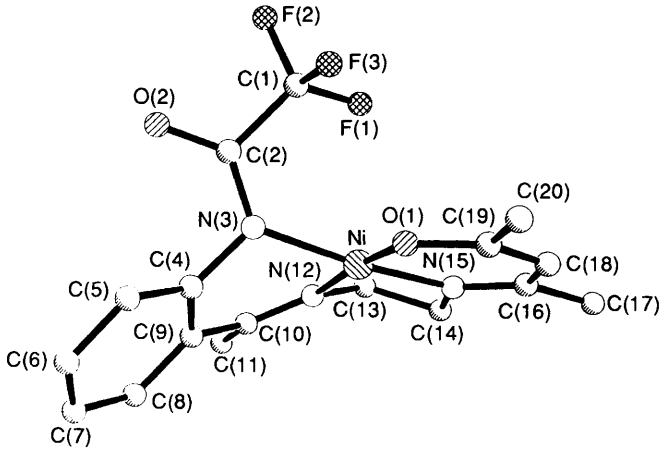

Fig. 4 A view of complex **5c** showing a nickel–fluorine interaction

Table 4 Structure determination summary for complex **5c**

Crystal data	
Empirical formula	$C_{17}H_{18}F_3N_3NiO_2$
M	412.04
Colour and habit	Red-brown prism
Crystal system, space group	Monoclinic, $P2_1/c$
Unit-cell dimensions	a = 9.057(2), b = 13.769(4), c = 14.664(4) Å, β = 108.43(2)°
U/Å^3, D_c/g cm^{-3}	1735.0(8), 1.581
Z, μ/cm^{-1}	4, 1.17
Data collection	
Scan type, 2θ range/°	ω, 3.5–55
Scan speed/° min^{-1}; scan range, ω/°	Variable, 3–15 in ω; 1.2
Background measurement	Stationary crystal and counter at beginning and end of scan, each for 25% of total scan time
Independent reflections	5078
Observed reflections	2836 [$F_o > 3\sigma(F_o)$]
Refinement	
System used	Siemens SHELXTL PLUS[13] (DIGITAL MicroVAX 3300)
Solution	Heavy-atom method
Refinement method	Full-matrix least squares
Quantity minimized	$\Sigma\omega\Delta F^2$
Hydrogen atoms	Riding model, U = 0.08 Å^2
Anisotropic parameters	Non-hydrogen atoms
Final R, goodness-of-fit, ω	0.0434, 1.26, 1
Data-to-parameter ratio	13:1
Maximum and minimum excursions/e Å^{-3}	+0.5 and −0.5

proton NMR spectrum of the ethylene fragment. As shown in Fig. 4, despite the planarity about the co-ordinated Ni atom, overall the molecule of **5c** is non-planar and hence chiral. Inversion of one of the enantiomers into the alternative one involves rotation about the Ni–N(3) bond along with associated rotations in the bonds of the six-membered chelate ring, causing the pendant trifluoroacetyl group to move to the other side of the ONNN plane. This motion is restrained to some extent by the additional interaction between the fluorine and nickel atoms, stabilizing each of the enantiomers and subsequently increasing the energy barrier for the inversion. Thus, it seems that the dynamic process monitored by proton NMR spectroscopy in the nickel complexes **4b** and **4c**, comprising a trifluoroacetyl pendant substituent, is the enantiomer interconversion inhibited by the Ni···F interaction. Accordingly, in the case of **4a**, wherein such a mode of enantiomer stabilization is not possible, no restricted dynamic process is observed down to −50 °C.

Experimental

Materials.—7-Amino-4-methyl-5-azahept-3-en-2-one **1** and 2-aminobenzaldehyde were prepared by the literature procedures.[1,12] *N*-Acetyl and *N*-trifluoroacetyl derivatives of 2-amino-benzaldehyde, -acetophenone and -benzophenone were obtained by acylation of the appropriate amino compound with acetic or trifluoroacetic anhydride, respectively. All other chemicals were reagent grade and used without further purification.

Ligands.—A solution of compound **1** (2.13 g, 0.015 mol) in methylene chloride (20 cm^3) was added dropwise to a refluxing solution containing 0.015 mol of 2-acetylaminobenzaldehyde, 2-trifluoroacetylaminobenzaldehyde, or 2-trifluoroacetylaminoacetophenone, respectively, in the same solvent (30 cm^3). The mixture was refluxed for 1 h, the solvent removed under reduced pressure, and the semi-solid residue recrystallized to give 9-(*o*-acetylaminophenyl)-4-methyl-5,8-diazanona-3,8-dien-2-one **4a** as soft white *needles* (3.66 g), from methanol–di-isopropyl ether, m.p. 82 °C [Found: C, 67.0; H, 7.4; N, 14.5%; M^+, 287 (100% in FD mass spectrum). $C_{16}H_{21}N_3O_2$ requires C, 66.9; H, 7.4; N, 14.6%; M, 287]; δ_H: 1.83, 1.88, 2.03 (s, H^{a,e,R^2}), 3.48 (q, H^g), 3.74 (t, H^h), 4.93 (s, H^c), 6.9–7.5 (m, $H^{l,m,n}$), 8.32 (s, H^{R^1}), 8.68 (d, H^o), 11.00 (br, H^f), and 12.34 (br, H^q).

4-*Methyl*-9-(o-*trifluoroacetylaminophenyl*)-5,8-*diazanona*-3,8-*dien*-2-*one* **4b**. Soft white *needles* from hexane (3.92 g), m.p. 88 °C [Found: C, 56.5; H, 5.3; N, 12.3%; M^+, 341 (100% in FD mass spectrum). $C_{16}H_{18}F_3N_3O_2$ requires C, 56.3; H, 5.3; N, 12.3%; M, 341]. δ_H: 1.90, 1.98 (s, $H^{a,e}$), 3.67 (q, H^g), 3.86 (t, H^h), 4.98 (s, H^c), 7.2–7.7 (m, $H^{l,m,n}$), 8.48 (s, H^{R^1}), 8.71 (d, H^o), 11.02 (br, H^f), and 14.12 (br, H^q).

4-*Methyl*-9-(o-*trifluoroacetylaminophenyl*)-5,8-*diazadeca*-3,-8-*dien*-2-*one* **4c**. Soft white *needles* from methanol (4.57 g), m.p. 130 °C [Found: C, 57.5; H, 5.7; N, 11.6%; M^+, 355 (100% in FD mass spectrum). $C_{17}H_{20}F_3N_3O_2$ requires C, 57.5; H, 5.7; N, 11.8%; M, 355]. δ_H: 1.98, 2.03, 2.41 (s, H^{a,e,R^1}), 3.67 (q, H^g), 3.79 (t, H^h), 5.02 (s, H^c), 7.0–7.6 (m, $H^{m,n}$), 7.75 (d, H^l), 8.74 (d, H^o), 11.05 (br, H^f), and 14.96 (br, H^q).

Nickel Complexes.—A solution of nickel(II) acetate tetrahydrate (0.62 g, 2.5 mmol) in methanol (20 cm^3) was combined with 2.5 mmol of ligand **4a**, **4b**, or **4c**, respectively, in methanol (30 cm^3). The mixture was stirred for 1 h at room temperature. The precipitated nickel complex was removed by filtration and recrystallized from methanol.

[9-(o-*Acetylaminophenyl*)-4-*methyl*-5,8-*diazanona*-3,8-*dien*-2-*onato*(2−)]*nickel*(II) **5a**. Bright-orange microcrystalline *solid* (0.67 g), m.p. 250 °C (Found: C, 56.1; H, 5.4; N, 12.2. $C_{16}H_{19}N_3NiO_2$ requires C, 55.9; H, 5.6; N, 12.2%). FAB mass spectrum:* m/z 344 (100), $[M + 1]^+$; 328 (9), $[M - CH_3]^+$; and 301 (19%), $[M + 1 - CH_3CO]^+$.

4-*Methyl*-[9-o-*trifluoroacetylaminophenyl*)-5,8-*diazanona*-3,8-*dien*-2-*onato*(2−)]*nickel*(II) **5b**. Dark-orange *prisms* (0.83 g), m.p. 258 °C (Found: C, 48.3; H, 4.1; N, 10.5. $C_{16}H_{16}F_3N_3NiO_2$ requires C, 48.3; H, 4.0; N, 10.6%). FAB mass spectrum: m/z 398 (100), $[M + 1]^+$; 328 (43) $[M - CF_3]^+$; and 301 (33%), $[M + 1 - CF_3CO]^+$.

[4-*Methyl*-9-(o-*trifluoroacetylaminophenyl*)-5,8-*diazadeca*-3,8-*dien*-2-*onato*(2−)]*nickel*(II) **5c**. Red-brown *prisms* (0.76 g), m.p. 300 °C (Found: C, 49.7; H, 4.4; N, 10.1. $C_{17}H_{18}F_3N_3NiO_2$ requires C, 49.6; H, 4.4; N, 10.2%). FAB mass spectrum: m/z 412 (100), $[M + 1]^+$; 342 (41), $[M - CF_3]^+$; and 315 (31), $[M + 1 - CF_3CO]^+$.

Physical Measurements.—Elemental analyses were performed on a Carlo Erba MOD 1106 elemental analyser. Field desorption mass spectra of the ligands (accelerating voltage

* Peaks related to the matrix and solvent are disregarded; m/z values reported for the most abundant ^{58}Ni isotope.

8 kV, extraction voltage −3 kV, emitter current 10 mA) were recorded on a Varian Mat 711 spectrometer. Fast atom bombardment mass spectra of the nickel complexes dissolved in dimethyl sulfoxide (dmso) were recorded using a *m*-nitrobenzyl alcohol matrix on a VG 30-250 spectrometer at the probe temperature; xenon was used as the primary beam gas and the ion gun operated at 8 kV and 100 μA. Proton NMR spectra of the ligands were run on a Tesla BS 567A 100 MHz spectrometer in $CDCl_3$ solution with $SiMe_4$ as internal reference, proton and ^{13}C NMR spectra of the complexes on a 300 MHz Nicolet spectrometer. The UV/VIS spectra were recorded on a Perkin-Elmer 402 spectrometer in methanol solution, and IR spectra (1000–4000 cm^{-1}) on a Perkin-Elmer 621 spectrometer in Nujol and hexachlorobutadiene mulls.

X-Ray Crystallography of Complex **5c**.—Material suitable for X-ray studies was obtained by slow infusion of methanol and diisopropyl ether to a solution of complex **5c** in methylene chloride. A roughly prismatic single crystal (maximum dimension 0.30 mm) was selected, mounted on a glass fibre, and transferred to a Siemens Nicolet R3m/V diffractometer for characterization and data collection, using Mo-Kα radiation (λ = 0.710 73 Å). No decomposition of the sample was observed during the exposure to X-rays. The space group and unit-cell dimensions were determined by least-squares refinement of 50 reflections at $2\theta > 30°$. An empirical absorption correction,[13] based on ψ scans of four reflections at $\chi \sim 90°$, was applied to the intensity data. Crystal data, data collection and refinement details are given in Table 4, while fractional atomic coordinates for non-hydrogen atoms and bond distances and angles are given in Tables 2 and 3, respectively.

Additional material available from the Cambridge Crystallographic Data Centre comprises H-atom coordinates and thermal parameters.

Acknowledgements

The authors gratefully acknowledge support from the Polish Scientific Research Council (KBN, Grant 1439) and from the National Science Foundation (Grant CHE 8102974).

References

1 E. Kwiatkowski and M. Kwiatkowski, *Inorg. Chim. Acta*, 1984, **82**, 101.
2 G. Cros and J. P. Costes, *C. R. Acad. Sci. Paris, Ser. II*, 1982, **294**, 173.
3 E. Kwiatkowski and M. Kwiatkowski, *Inorg. Chim. Acta*, 1986, **117**, 145.
4 M. Kwiatkowski, E. Kwiatkowski, A. Olechnowicz, D. M. Ho and E. Deutsch, *J. Chem. Soc., Dalton Trans.*, 1990, 3063.
5 J. P. Costes, G. Cros, M. H. Darbieu and J. P. Laurent, *Inorg. Chim. Acta*, 1982, **60**, 111; J. P. Costes, *Inorg. Chim. Acta*, 1987, **130**, 17.
6 R. C. Coombes, J. P. Costes and D. E. Fenton, *Inorg. Chim. Acta*, 1983, **77**, L173; J. P. Costes and M. I. Fernandez-Garcia, *Transition Met. Chem.*, 1988, **13**, 131.
7 C. J. Pouchert, *The Aldrich Library of NMR Spectra*, 2nd edn., Aldrich Chemical Company, Milwaukee, WI, 1983, vol. 2, pp. 333–339.
8 L. Sacconi, P. Nannelli and U. Campigli, *Inorg. Chem.*, 1965, **4**, 818; A. B. P. Lever, *Inorganic Electronic Spectroscopy*, Elsevier, Amsterdam, 1968, p. 343.
9 A. Bondi, *J. Phys. Chem.*, 1964, **68**, 441.
10 E. Kwiatowski and M. Kwiatkowski, *Inorg. Chim. Acta*, 1980, **42**, 197.
11 M. Kwiatkowski, E. Kwiatkowski, A. Olechnowicz, D. M. Ho, and E. Deutsch, *J. Chem. Soc., Dalton Trans.*, 1990, 2497 and refs. therein; F. Akhtar and M. G. B. Drew, *Acta Crystallogr., Sect. B*, 1982, **83**, 1149 and refs. therein.
12 L. J. Smith and W. J. Opie, *Org. Synth. Collect.*, 1956, **3**, 56.
13 W. Robinson and G. M. Sheldrick, in *Crystallographic Computing*, eds. N. W. Isaacs and M. R. Taylor, Oxford University Press, 1988, vol. 4, p. 366.

Received 20*th May* 1991; *Paper* 1/02362D